Article   **Open Access**

Characteristics and close-range exploration methods of near-Earth asteroid 2016HO$_3$

He Zhang, Fei Li*, Linzhi Meng, Fuming Zeng, Xiaoyu Jia, Yu'ang Liu

Beijing Institute of Spacecraft System Engineering, *Beijing* 100094, *China*

*Correspondence: kuokuolee@163.com

Abstract: The characteristics of asteroids are vital parameters for planning asteroid exploration missions. These characteristics have been explored in close range for some typical asteroids, and are summarized in the article. This allows estimates of the characteristics of asteroid 2016HO$_3$, the target of the first Chinese asteroid exploration mission, Tianwen 2. We obtain 80 characteristic parameters in 9 categories and analyze their impacts on the mission. By comparing three close-range exploration modes, we provide advantages and disadvantages of each, and propose suitable methods for the exploration of 2016HO$_3$. Owing to the weak gravity and small size of 2016HO$_3$, a combination of multiple hovering positions and active orbiting is recommended for scientific exploration.

Keywords: Near-Earth asteroid; 2016HO$_3$; Tianwen 2; Close-range exploration; Characteristics

1. INTRODUCTION

Celestial bodies in our solar system are classified into three categories: planets, dwarf planets, and small solar system bodies (SSSB)[1]. SSSB include asteroids, comets, interplanetary dust particles, and other interplanetary matter. Asteroids, also referred to as minor planets, are celestial bodies that orbit sun. They are smaller than planets and dwarf planets in size and mass, and are less likely to release gas and dust[2]. They are sometimes referred to as "living fossils" in solar system research, because their low degree of evolution means that the environmental conditions of the solar system's formation and evolution are preserved in them. In addition, asteroids may contain important clues to the origin of life and water on Earth, and the possibility of impact events may have potential effects on Earth's environment. Consequently, exploring asteroids is a valuable endeavor. Since the 1990s, asteroid missions have been increasing as asteroid exploration has become an important research topic, and fruitful results have been achieved.

A series of asteroid exploration missions have been launched, with exploration methods including flyby, such as Deep Space 1, Stardust, and Rosetta; orbital exploration, such as Near Earth Asteroid Rendezvous (NEAR) and Dawn; in-situ exploration such as Rosetta; sample return, such as Stardust, Hayabusa 1, Hayabusa 2, and OSIRIS-REx; asteroid impact missions, such as the dual asteroid redirection test (DART)[3].

The Tianwen 2 asteroid exploration mission is a milestone in Chinese planetary exploration, beginning at a high technical level. Tianwen 2 aims to complete a close-range exploration and sample return for the near-Earth asteroid (NEA) 2016HO$_3$, and close-range exploration of a main belt comet, 311P, in a single mission. The overall mission is expected to yield breakthroughs in key technologies, obtain new scientific achievements, enhance China's space travel technology, and prompt leapfrog development of Chinese deep space exploration [4].

The target characteristics of asteroids are important inputs for designing an asteroid mission. Here, we summarize the characteristics of typical asteroids already explored, analyze the characteristics of the 2016HO$_3$, and examine close-range exploration methods for 2016HO$_3$.

2. CHARACTERISTICS OF TYPICAL SMALL BODIES

Summarizing the characteristics of six asteroids explored by NEAR, Hayabusa 1, Hayabusa 2, and OSIRIS-REx (see Table 1 and Fig. 1, 2), we reach the following conclusions:

(1) Structure: Four near-Earth asteroids have "rubble-pile" structures, and two large main belt asteroids have melt-differentiation structures. A rubble-pile is an asteroid that is not a monolith, consisting instead of numerous pieces of rock that have coalesced under the influence of gravity. Differentiated asteroids are inferred to be objects, or fragments of objects, that were once heated to

Table 1. Summary table of the characteristics of typical asteroids[5–8]

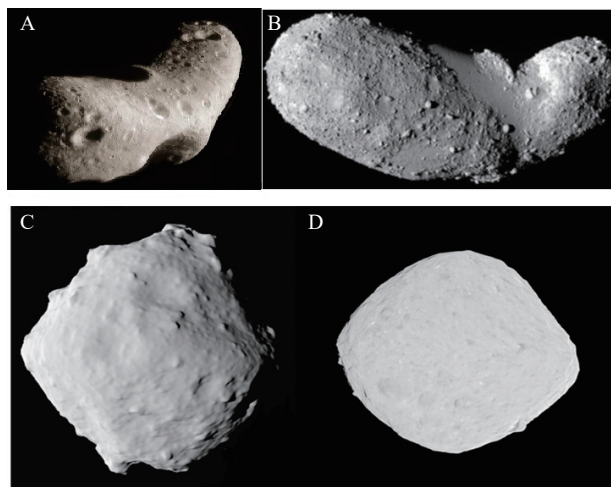| Missions	Asteroid	Shape /km	Density /(g/cm³)	Mass /kg	Structure	Spectral category	Meteorite category	Surface topographic features	Surface mechanical characteristics	Temperature /K	Thermal inertia /(Jm⁻²s⁻⁰·⁵K⁻¹)	Geometric albedo	Rotation period /h	Direction of rotation
NEAR	Eros: NEA	34×11×11	2.67±0.03	$6.687×10^{15}$	Rubble piles. Porosity: 21%~33%	S	L ordinary chondrite	● The ratio of depth and diameter is 0.12, lacking > 100 m craters ● With wide grooves and mountains ● Average slopes: 8°~10° ● Surface particle characteristics: The thickness of the regolith is estimated to be over 10 m, and the particle size of the regolith is approximately 50–100 μm	/	123–373	150	0.33 ±0.03	5.27	prograde
Hayabusa 1	Itokawa: NEA	0.535×0.294×0.209	1.9±0.13	$3.58×10^{10}$	Rubble piles. Porosity 41%	S	LL ordinary chondrite (LL5 or LL6)	● The ratio of depth and diameter is 0.08, lacking > 100 m craters ● There is a group of mountains that have no obvious connection to the impact crater ● Rocks power index: ~3.1 ± 0.1 ● The surface is divided into rough and smooth areas, with rough areas covered by boulders and no regolith below 1cm. The smooth area has regolith with a thickness of about 2.5 m and a particle size greater than 1 mm	adhesive strength is about 100 Pa	217–445	700	~0.53	12.13	retrograde
Hayabusa 2	Ryugu: NEA	1.04×1.02×0.88	1.19±0.02	$4.5×10^{11}$	Rubble piles. Porosity 50%	B	CM, CR, CI Carbonaceous chondrite	● Rock distribution: More than 4400 stones >5 m on the 2.7 km² surface of Ryugu; More than 97800 stones >2 m. There are slight differences in the number of stones at different latitudes and longitudes. The number of stones above 20 m is twice that of Bennu and Itokawa, and the maximum number of stones reaches 140 m ● Rock Power index (above 5 m): ~2.65 ± 0.05 ● Particle distribution: The surface is mainly composed of stones on the order of centimeters or even larger ● Difficult to find a flat area with a radius of 50 m	Surface adhesive strength<1.3 Pa; subsurface adhesive strength:140~670 Pa	300–370	247–375	0.045± 0.002	7.63	retrograde
Dawn	Ceres: Main belt asteroid	965.2×961.2×891.2	2.161	$9.39×10^{20}$	melt-differentiation structure	C	Carbonaceous chondrite	● The surface is covered with numerous impact craters, but the diameter is less than 280 km ● Surface protrusions are not obvious	/	168 (Average)	50–60	0.090± 0.0033	9.07	prograde
Dawn	Vesta: Main belt asteroid	672.6×557.2×446.4	3.513	$2.67×10^{20}$	melt-differentiation structure	V	HED meteorite	● The surface presents an extremely diverse group of impact craters with strong undulations ● An impact crater with a diameter of several dozens of km, partially covered by ejecta ● Regolith thickness: estimated to reach several km ● Slope: up to 55° maximum	/	85–270	30±10	~0.423	5.34	prograde
OSIRIS-REx	Bennu: NEA	0.564×0.536×0.498	1.19	$7.33×10^{10}$	Rubble piles. Porosity 50%~60%	B	CM Carbonaceous chondrite	● Equatorial uplift, towering north-south ridges ● The surface is covered with pebbles and boulders, with over 200 boulders with a diameter exceeding 10 m, some of which can reach a diameter of 30 m, and many craters with a length of 10–150 m ● Rock power index (above 8m): ~2.9 ± 0.3 ● Average slope: 17°±2° ● Difficult to find a flat area with a radius of 25 m	/	200–350	350±20	~0.046	4.30	retrograde

Fig. 1. (A) Shapes of the asteroids Eros. (B) Itokawa. (C) Ryugu. (D) Bennu .
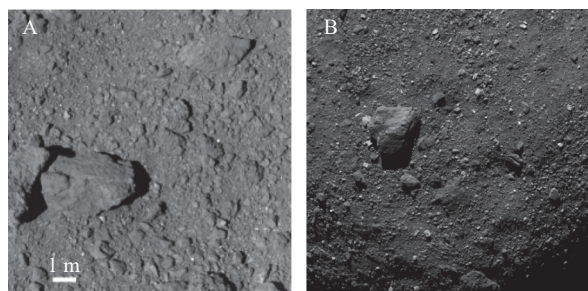

Fig. 2. (A) Surface images of Ryugu and (B)Bennu, showing size variation of surface rocks[7].

the point of partial melting, showing geochemical segregation of their component materials.

(2) Shape: All have irregular and significantly different shapes.

(3) Rotation: The rotation period slows down with increasing diameter, ranging from 4.30 hours to 12.13 hours. The direction of rotation includes both prograde and retrograde (i.e., where orbital revolution and asteroid rotation directions are the same and opposite, respectively), and there is significant variation in the alignment of the rotational axis.

(4) Relation to meteorite types: C-type asteroids (Ryugu, Bennu, and Ceres) correspond to carbonaceous chondrites, while S-type asteroids (Eros and Itokawa) correspond to ordinary chondrites.

(5) Mechanical properties: These properties have only been directly measured for two target asteroids. The surface layer of Ryugu is composed of rubble with weak adhesive strength (<1.3 Pa), and the subsurface layers are composed of smaller particles with higher adhesive strength (140−670 Pa). The adhesive strength of the surface layer of Itokawa is approximately 100 Pa. Surface mechanical properties among different targets vary significantly.

(6) Rock distribution: Rocks on asteroid surfaces are of varying sizes, including regolith, pebbles, and boulders. Generally, the greater the gravitational force of an asteroid, the smaller the surface particle size is. Itokawa, the smallest asteroid that has been closely explored, has a regolith layer of 1 mm sized particles with a thickness of

about 2.5 m.

(7) Temperature: The surface temperature changes significantly on an individual asteroid, from several tens to hundreds of Kelvin.

(8) Albedo: Asteroids generally have a low albedo. The albedo of C-type asteroids is lower than that of S-type.

(9) Surface topography: Asteroids show a combination of impact craters, boulders, regolith, pebbles, and linear structures (such as grooves), with complex terrain and fewer locally flat areas.

3. CHARACTERISTICS OF 2016HO$_3$

The revolution period of the NEA 2016HO$_3$ is very similar to that of Earth, placing it among the 1:1 co-orbiting bodies of Earth. From a geocentric view, this asteroid travels along an approximately circular trajectory in a persistent and stable near-Earth orbit (Fig. 3), hence it is also known as a quasi-satellite of the Earth. 2016HO$_3$ is the fifth Earth quasi-satellite and currently the closest and most stable one. 2016HO$_3$ is the provisional designation, and 469219 is the catalog number. 2016HO$_3$ is also named Kamo'oalewa, a Hawaiian word that refers to an oscillating celestial object.
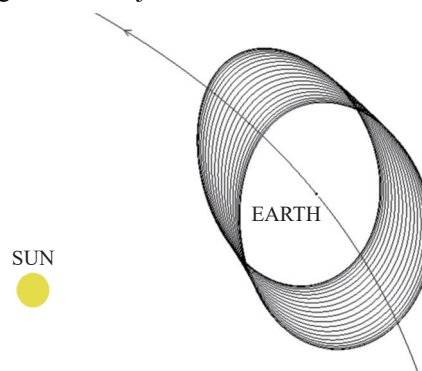

Fig. 3. Illustration of the orbit of asteroid 2016HO$_3$ in Earth's rotating frame.

The Tianwen 2 mission will complete an approach, rendezvous, close-range exploration, and sampling of 2016HO$_3$. The mission will collect data for a total of 80 parameters in 9 categories for 2016HO$_3$, including orbit, photometry, spectrum, volume, morphology, rotation, thermal characteristics, surface characteristics, and environment (refer to satellite, dust). The parameters involved in each stage of the mission are shown in Table 2.

2016HO$_3$ is a dim target, with an apparent magnitude varying between 22.5 and 25.5 in ground observations, so observational information is very limited. The following will explain the main characteristics that have a significant effect on the mission, such as orbit, photometry, spectrum, volume, morphology, rotation, thermal characteristics, surface characteristics, and environment, based on limited observation information and inference[9].

3.1. Orbit

The revolution period of 2016HO$_3$ is approximately

Table 2. Mission requirements for the targeted characteristic parameters of 2016HO$_3$

Categories	Parameters	Requirements	Importance/normal
Orbit	Orbital elements	Orbit design, target capture strategy design	important
	Orbital uncertainty	Target capture strategy design	important
Photometry	Brightness	Target capture, navigation sensor/payload camera in orbit operating conditions	important
	Phase function		important
	Color index	Inferring Spectral types and similar meteorites Indirect effect on sampling design	normal
Spectrum	Spectrum	Determine the corresponding meteorite type Indirect effect on sampling design	normal
	Categorize		normal
	Similar meteorite		normal
Volume	Diameter	Close-range exploration flight strategy, relative navigation, sampling design	important
	Shape	Close-range exploration flight strategy, relative navigation, sampling	important
	Gravitation	Design of control strategies for close-range detection, descent, and sampling processes	normal
Morphology	Morphology(rock distribution, crater distribution, etc.)	Design of relative navigation and sampling strategies	important
Rotation	Rotation period	Design of close-range exploration flight strategy and relative navigation strategy	important
	Direction of the rotation axis, the direction of rotation, non-principal axis rotation		important
Thermal	Thermal inertia, etc	Design of close-range exploration and sampling strategies	important
	Surface temperature		important
	Albedo	Design of close-range exploration strategy, analysis of thermal environment for sampling, adaptive design of navigation sensors/payload cameras	important
Surface characteristics	Surface mechanical properties	Sampling mission design	important
	Surface electrical properties	Analysis of the communication link between the sampling process and the ground The sampling work needs to be completed independently by the detector, and communication during this stage has little effect on the mission	normal
Environment	Nature satellites	Design of close-range exploration strategies	normal
	Dust	Sampling Adaptability of mechanisms, navigation sensors/payload cameras, etc.	normal

1 year, with the distance between 2016HO$_3$ and the sun varying between 0.89 AU and 1.10 AU, while its distance from Earth varies between 16 million km and 44 million km[10].

3.2. Photometry

Absolute magnitude represents the brightness of a target body under unified observation conditions. For 2016HO$_3$, the absolute magnitude is 24.3, corresponding to a dim target. The phase function can characterize the brightness changes of 2016HO$_3$ at different phase angles (observer-2016HO$_3$-solar angle), using the H-G function with $G = 0.15$ [11,12]. H corresponds to the mean V-band magnitude, at a 0° phase angle (i.e., the absolute magnitude), and G is the so-called slope parameter, which describes the shape of the magnitude phase function. The phase angle and magnitude of 2016HO$_3$ are shown in Fig. 4, and the phase function of 2016HO$_3$ is shown in Fig. 5.
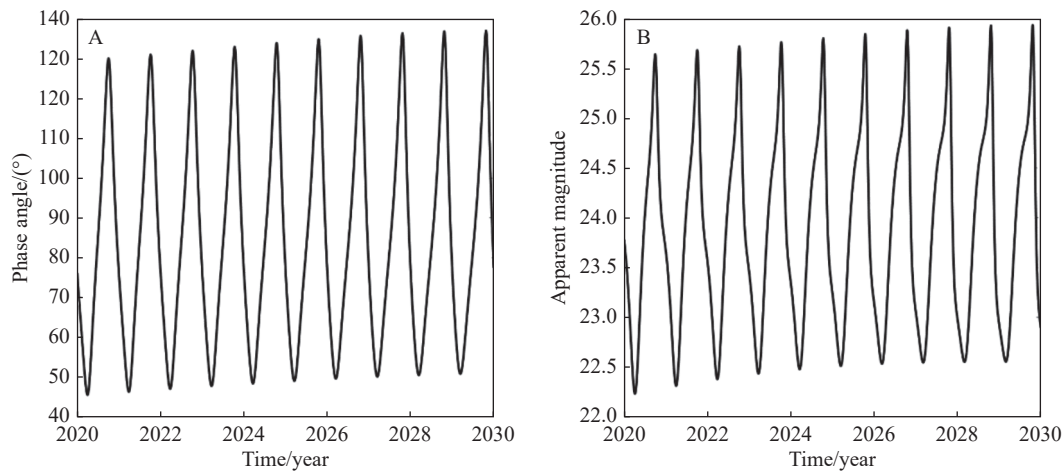

Fig. 4. (A) Phase angle (solar-asteroid-earth angl) and (B) apparent magnitude of asteroid 2016HO$_3$ between 2020 and 2030.

3.3. Bulk Characteristics

According to spectral analysis, 2016HO$_3$ is an S-type asteroid with a density ranging from 1.2 g/cm^3 to 3.3 g/cm^3. According to the maximum envelope, the diameter of 2016HO$_3$ varies from 30 m to 100 m[12, 13]. The gravitational field of 2016HO$_3$ is weak, with the gravitational parameters detailed in Table 3, and can be regarded as a microgravity environment.

According to the light curve (shown in Fig. 6), the shape of 2016HO$_3$ can be inferred to be elongated. Assuming that 2016HO$_3$ is a three-axis ellipsoid with axis
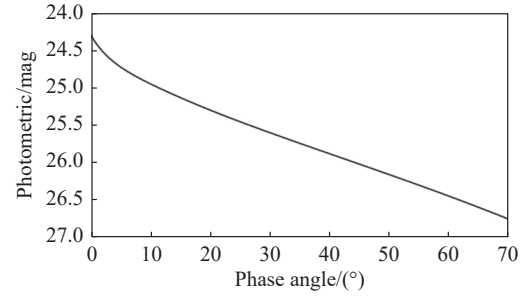

Fig. 5. Phase function of asteroid 2016HO$_3$.

lengths of a, b, and c ($a \geqslant b \geqslant c$), we determine that $a/b \geqslant$ 2.1 and $b/c \geqslant 1$.

Table 3. 2016HO$_3$ volume, mass, and gravity parameters

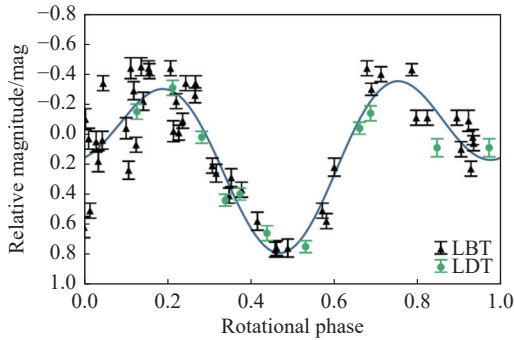| Parameter	Formula	Result
Volume	$V = \dfrac{4}{3}\pi R^3$	$V = 1.41 \times 10^4 - 5.24 \times 10^5$ m^3
Mass	density × volume	$M = 1.7 \times 10^7 - 1.7 \times 10^9$ kg
Hill sphere radius	$R_H = \sqrt[3]{M/3M_\odot}\, q$ M is the mass of 2016HO$_3$, $M_\odot$ is the mass of the sun, q is perihelion distance	$R_H = 1.9 - 8.9$ km
Gravitational acceleration	Spherical asteroid $g = GM/R^2$	$g = 5.0 \times 10^{-6} - 4.6 \times 10^{-5}$ m/s^2
Escape speed	$v_p = (2GM/R)^{0.5}$	$v_p = 1.2 - 6.8$ cm/s

Fig. 6. Light curve of 2016HO$_3$[14].

3.4. Rotation

The average rotation period of 2016HO$_3$ is determined using the light curve (Fig. 6) to be approximately 28±0.48 minutes[13,14]. The direction of the rotational axis is still unknown[13,14].

3.5. Thermal Characteristics

(1) Geometric albedo

Geometric albedo is the ratio of the brightness of an asteroid to the brightness of a completely diffuse reflective surface with the same cross-sectional area. As an S-type asteroid, the geometric albedo range for 2016HO$_3$ is 0.1−0.3 [5].

(2) Thermal inertia

Thermal inertia can reflect the surface morphology of asteroids, and larger particle size of the regolith on the surface of a small body causes greater thermal. There is an approximate relationship between the asteroid diameter (D) and their thermal inertia (Γ): $\Gamma = d_0 D^{-\xi}$, $d_0 = 300 \pm$

47 Jm^{-2}s$^{-0.5}$K^{-1}, $\xi = 0.48 \pm 0.04$[15].

For an object with a diameter of 30−100 m, the thermal inertia is between 900 and 1600 Jm^{-2}s$^{-0.5}$K^{-1}. The larger the thermal inertia, the smaller the temperature fluctuation on the surface of the asteroid, leading to a milder thermal environment. Therefore, the design focuses on the lower limit of the thermal inertia of 2016HO$_3$. From an engineering design perspective, because the thermal inertia of the lunar surface is 40 Jm^{-2}s$^{-0.5}$K^{-1}, so the lower limit of thermal inertia for 2016HO$_3$ is considered to be the same.

3.6. Morphology

The surface morphology of asteroids is rich and diverse, including features such as smooth or rough surfaces, steep slopes, millimeter-sized particles to meter-sized boulders, and impact craters with a wide range of scales. The size and distribution of rocks, as well as surface topography, are crucial for sampling. Due to limitations in observation capabilities, detailed analysis of surface morphology can only be carried out after obtaining high-resolution images of the surface through close-range detection. Based on the results of asteroid exploration missions, analogical analysis is conducted on the surface morphology of 2016HO$_3$.

(1) Structure

There is still debate over whether 2016HO$_3$ is a monolith or a rubble pile.

(2) Surface topography

There are numerous ridges, grooves, and craters distributed on the surfaces of asteroids, causing their undulating terrain, and there are significant differences in sur-

face topography between different individuals.

(3) Rock size and distribution

The surface rocks of asteroids are categorized as regolith and boulders, as shown in Table 4. Due to the lack of clear size criteria for these categories, this article defines regolith as a mixture of stones and dust, while boulders are defined as stones with a diameter greater than a meter.

Table 4. Typical rocks on the surface of asteroids[5]

Category	Characteristic	Image
Boulders	Structurally intact, with fractures or edges	
Regolith	A mixture of small stones and dust	

Regolith: There is regolith on the surfaces of Itokawa, Ryugu, Bennu, and Eros, with a thickness of approximately 2.5 m for Itokawa[16] and over 30 m for Eros[17]. The regolith layer thickness may range from millimeters to centimeters on the surface of 2016HO$_3$, and it is highly likely to exist in polar and high-latitude regions.

Boulders: Larger asteroids have correspondingly larger boulders with a greater number density. The maximum diameter of Itokawa and Bennu are both on the order of 500 m, and the largest observed boulder on them is approximately 50 m in size. The diameters of Ryugu and Eros are on the order of kilometers, with a maximum boulder size of around 160 m. The average number density of boulders with a diameter greater than 20 m in areas between 70° N and 70° S on Ryugu is 50 km^{-2}, and the corresponding number of boulders on Itokawa is only half that of Ryugu.

According to observation data of multiple asteroids, the power-law distribution can be used to describe the integrated frequency of surface rocks on asteroids, given by

$$N = AD^{-\xi}, \tag{1}$$

where N is the expected number of rocks larger than D per unit area, D is the size of the rock, ξ is a power exponent, and A is a constant related to the asteroid.

The rocks on the surfaces of asteroids are subject to long-term bombardment by micrometeorites, solar wind, ion irradiation from cosmic rays, and temperature fluctuations, resulting in changes in their surface structure. Analysis shows that rocks on the surfaces of asteroids are likely to be rough.

Based on the power-law distribution of stones on Itokawa and Ryugu[13,14], the number of rocks larger than 5 m on the surface of 2016HO$_3$ can be calculated (the estimated diameter of 2016HO$_3$ is 30−100 m). Results indicate that there may be a number of boulders larger than 5 m on the surface of 2016HO$_3$, as shown in Table 5. The surfaces of boulders may be coated in a layer of regolith due to long-term space weathering.

Table 5. Estimated number of surface stones on 2016HO$_3$

Referenced asteroid	Number of rocks larger than 5 m
Itokawa	2.8−31.4
Ryugu	4.6−51.2

3.7. Surface Mechanical Properties

(1) Rock compressive strength

The upper limit of compressive strength for bedrock with monolith structure or surface rock with a rubble-pile structure is likely to be less than 200 MPa. According to the test results of the compressive strength of S-type meteorites collected on Earth, the compressive strength of 2016HO$_3$ rocks is between 20 MPa and 200 MPa.

(2) **Surface strength of 2016HO$_3$**

A simulation analysis has been conducted on the relationship between the adhesive strength and compressive strength of the surface regolith of 2016HO$_3$, with results showing that the compressive strength is significantly

affected by the adhesive strength between particles:

● If the adhesive strength of the surface regolith is 0, the surface compressive strength is only several tens of Pa;

● If the cohesive strength of the surface regolith is 30 Pa, the surface compressive strength can reach several kPa[18].

If $2016HO_3$ has a rubble-pile structure, its rotation period is only 28 minutes, giving an estimated surface cohesive strength on the order of 30 Pa or above, as shown in Fig. 7.

Under the worst of circumstances, the surface compressive strength of $2016HO_3$ can reach several tens of Pa, and it is likely to reach several kPa.

3.8. Summary of Target Characteristics

The conclusion of important target characteristics and their effect on the mission are shown in Table 6.

4. MODE DESIGN FOR CLOSE-RANGE EXPLORATION

Japan Aerospace Exploration Agency (JAXA) and National Aeronautics and Space Administration (NASA) have advanced steadily in the exploration and modeling of small bodies. NASA also obtained 111 physical characteristic parameters of Bennu through multiple ground-
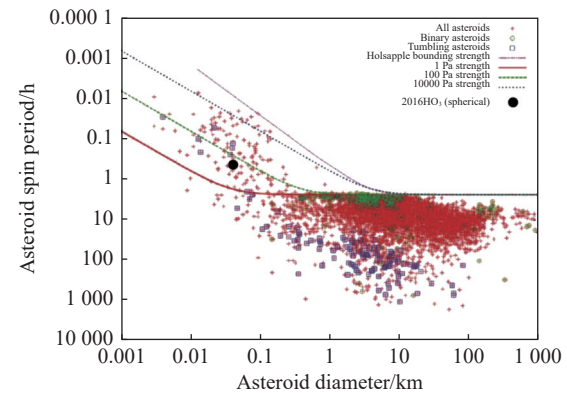

Fig. 7. The relationship between the diameter of asteroids and their rotational speed. The horizontal axis represents the asteroid diameter and the vertical axis represents the spin period. Different curves represent different bonding strengths between particles[5].

based radar/optical telescopes and space-based telescopes before launching OSIRIS-REx. However, Hayabusa 2 and OSIRIS-REx detected that the abundance of boulders on the surface of the target small bodies greatly exceeded expectations, making it difficult to find sampling areas meeting their requirements. Therefore, detection and navigation control strategies were adjusted based on in-orbit modeling results.

For the Tianwen 2 mission, accurate characteristic parameters of $2016HO_3$ cannot be obtained before launch.

Table 6. $2016HO_3$ important target characteristic parameters

Target	Characteristic	Reliability	Result	Mission effect analysis
Orbit	Orbital elements	High	The orbit parameters are obtained, with a positional uncertainty of approximately 120 km (1 σ)	Affects the orbit design, probe approach, and rendezvous
	Orbital uncertainty	High		
Photometry	Absolute magnitude	High	24.3	Design input of navigation sensor for target capture capability and indicators
Rotation	Spin period	High	About 28 min	Affects the design of close-range detection strategies and needs to adapt to different rotation axis directions
	Direction of the rotation axis	Low, requires precise measurement in orbit	Unknown, the rotation axis is more likely to approach the direction perpendicular to the orbital plane	
Volume	Diameter	Medium, uncertainty has little effect on missions	The diameter is 30−100 m, and the shape is relatively slender	Shape and size affect the design of close-range hovering positions and flight strategies
	Shape	Low, requires precise measurement in orbit		
Morphology	Surface topography	Low, requires precise measurement in orbit	The surface topography of $2016HO_3$ is complex, and there may be a regolith of rock ranging from millimeters to centimeters in size. At the same time, there may also be boulders larger than meters with rough surfaces	Affects sampling strategy design
	Rock size and distribution			
Thermal characteristics	Geometric albedo	Medium, requires precise measurement in orbit	0.1−0.3	Design input of navigation sensor and camera
	Thermal inertia		>40 Jm^{-2} s$^{-0.5}$K^{-1}	Main inputs for thermal environment analysis
Surface mechanical properties	Rock strength	Low, requires precise measurement in orbit	$2016HO_3$ bedrock (surface rock) strength 20−200 MPa	Need to be able to attach samples to the rock surface
	Surface strength	Low, requires precise measurement in orbit	>30 Pa	Preventing sinking during the sampling process

Scientific goals and sampling tasks must be supported by in-orbit data obtained from close-range exploration, such as characteristic parameters and feature models.

The close-range exploration of small bodies differs greatly from the exploration of larger celestial bodies such as the moon and Mars. The gravitation of large celestial bodies is strong, so that probes can enter a stable orbit of the celestial body at altitudes of hundreds of kilometers, and payloads are used for remote sensing. Due to the much weaker gravity of small bodies, the altitude of a stable orbit is extremely low. Consequently, the altitudes and types of the close-range exploration orbits can be changed at the cost of only minor velocity increments.

The design principles for the close-range exploration of 2016HO$_3$ mainly include two aspects. First, flight safety must be guaranteed. Second, the velocity increment should be as low as possible. The main modes of close-range exploration include hovering, active orbiting, and natural orbiting. Active orbiting and hovering are accomplished through orbital maneuver strategies at the cost of fuel consumption. Natural orbiting relies on external forces such as gravity or solar pressure, which can reduce the frequency of orbital maintenance and reduce fuel consumption. The specific instructions for each mode are as follows.

(1) Hovering

Hovering means that the position of the probe remains unchanged relative to the orbital coordinate system of the target small body, with a relative velocity of zero. Position maintenance is implemented when the position or speed exceeds the expected range.

The Hayabusa 1 and Hayabusa 2 spacecraft used hovering due to the small size of their targets. As shown in Fig. 8, the hovering altitude of was gradually decreased from 20 km to 10 km, then to 3 km, and finally to 0 km. Physical and morphological characteristics can be determined by observing the rotation of the target.
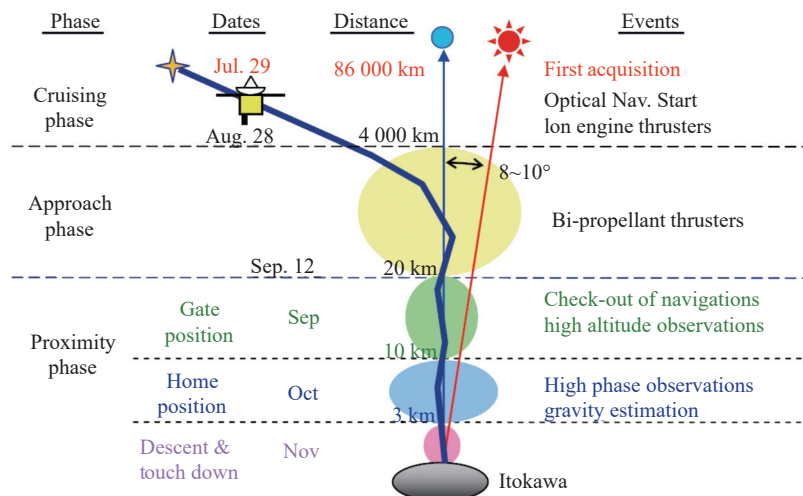

Fig. 8. Illustration showing varying hovering altitudes of Hayabusa 1.

Hovering can ensure little change in illumination conditions at the sub-satellite point, providing relatively consistent detection conditions for the sensor, which benefits relative navigation and autonomous control. Alternatively, remote sensing images with relatively consistent illumination conditions can be obtained through the rotation of the target celestial body. Frequent position maintenance is required for hovering mode, requiring a specific velocity increment of approximately 0.1 m/s per day.

(2) Active orbiting

Active orbiting means that the probe orbits near the small body along a predetermined trajectory. The position and velocity relative to the small body are changed by orbital maneuvers. This was used by the OSIRIS-REx mission at a relatively long distance (Fig. 9) to determine physical and morphological characteristics.

Active orbiting is relatively flexible at the cost of a certain velocity increment of approximately 1 m/s per day.
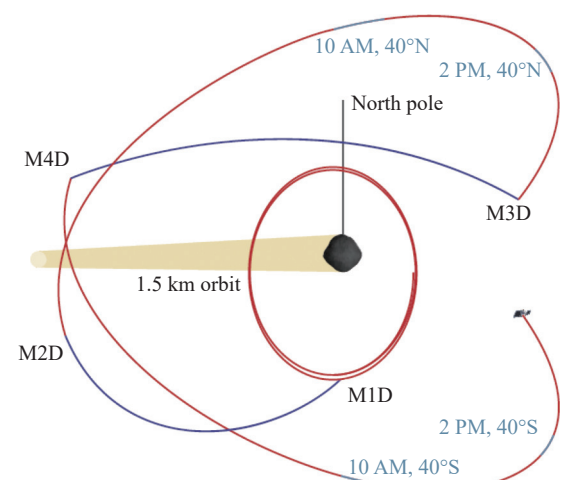
(3) Natural orbiting

Fig. 9. Illustration showing active orbiting trajectory of OSIRIS-REx.

In natural orbiting, the spacecraft behaves like a satellite of the target celestial body. To be stable, these orbits use natural forces such as gravitational pull or solar pressure, and active control is not necessary to maintain the orbit. Consequently, few velocity increments are required. However, stable natural orbits are more likely to be dawn-dusk orbits, resulting in poor illumination conditions at the sub-satellite point, which is not conducive to autonomous navigation or scientific investigation.

The OSIRIS-REx mission used data obtained by active orbiting at a relatively high altitude to determine that a natural orbit at an altitude of $1-1.5$ km could be achieved using the gravity of Bennu and solar wind pressure.

The gravity of $2016HO_3$ is weak and the altitude of a natural orbit is about $50-100$ m, which is close to the radius of $2016HO_3$, meaning there may be a risk of collision. Therefore, scientific detection and mapping is best achieved with a combination of multiple hovering positions and active orbiting. $2016HO_3$ is a small asteroid with a fast rotation speed. Accordingly, hovering mode can easily obtain high overlap images using rotational characteristics, reducing propellant consumption. In summary, hovering is the preferred mode for the Tianwen 2 mission, supplemented by active orbiting in areas with poor navigation conditions.

5. CONCLUSION

This article summarizes the characteristics of six asteroids obtained by successful asteroid missions, highlighting significant differences between them. For asteroids that have been sampled (Ryugu and Itokawa), their surface mechanical properties can be inferred, although similar data are still unknown for other asteroids that have only been explored through orbital observations.

Analyzing the characteristics of the NEA $2016HO_3$, the target of Tianwen 2, important parameters, such as orbit, luminosity, bulk characteristics, rotation, thermal characteristics, surface morphology, and surface mechanics, can be explained.

(1) Characteristic parameters such as orbit, luminosity, and rotation period are clarified, which can support effective mission design.

(2) Characteristic parameters such as size, shape, rotation axis direction, and surface morphology cannot be determined via ground-based observations, and only the maximum range is currently available. The exploration strategy needs to be planned to cover the maximum range of parameters in order to reduce the impact of any uncertainties. Characteristic parameters can be further determined based on close-range examination from orbit, and corresponding strategies can be developed.

(3) The surface mechanical properties of the target cannot be determined, and contain a high level of uncertainty, causing a significant impact on planning a sampling mission. The mission design should therefore be carried out according to the most likely surface mechanical properties.

Finally, a comparative analysis has been conducted on the three main modes used for close-range exploration of asteroids: hovering, active orbiting, and natural orbiting. Owing to the weak gravity of $2016HO_3$, the low altitude of its natural orbits carry a risk of collision, so a combination of multiple hovering positions and active orbiting is the most effective strategy to use. From the perspective of scientific detection and minimizing propellant usage, hovering is preferred, with supplemental active orbiting best employed in areas with poor navigation conditions. Further research will be conducted to determine hovering positions for close-range exploration in the future.

AUTHOR CONTRIBUTIONS

He Zhang conceived the idea and played the project administration and supervision role. Fei Li mainly wrote the original draft and provided methodology. Linzhi Meng provided investigation support and Fuming Zeng conducted validation work. Xiaoyu Jia prepared data curation. Yu'ang Liu performed formal analysis. Both Xiaoyu Jia and Yu'ang Liu reviewed and edited the manuscript. All authors read and approved the final manuscript.

DECLARATION OF INTERESTS

He Zhang is an editorial board member for Astronomical Techniques and Instruments and was not involved in the editorial review or the decision to publish this article.The authors declare no competing interests.

REFERENCES

[1] International Astronomical Union (IAU). 2006. IAU 2006 general assembly: results of the IAU resolution votes. https://www.iau.org/news/pressreleases/detail/iau0603/#3.

[2] GB/T 30114.4-2014. 2013. Terminology for space science and application—Part 4: lunar and planetary science. Beijing: Standards Press of China.

[3] Zhang, R. Q., Huang, J. C., He, R. W., et al. 2019. The development overview of asteroid exploration. *Journal of Deep Space Exploration*, **6**(5): 417−423. (in Chinese)

[4] The State Council Information Office of the People's Republic of China. 2022. China's space program: a 2021 perspective. https://www.doc88.com/p-74459799572504.html.

[5] Michel, P., DeMeo, F. E., Bottke, W. F. 2015. Asteroid IV. Tucson: The University of Arizona Press.

[6] Tatsuhiro, M., Nakamura, A. M., Hirata, N. 2010. The shape distribution of boulders on Asteroid 25143 Itokawa: Comparison with fragments from impact experiments. *Icarus*, **207**: 277−284.

[7] Lauretta, D. S., Dellagiustina, D. N., Bennett, C. A., et al. 2019. The unexpected surface of asteroid (101955) Bennu. *Nature*, **568**(7750): 55−60.

[8] Sugita, S., Honda, R., Morota, T., et al. 2019. The geomorphology, color, and thermal properties of Ryugu: implications for parent-body processes. *Science*, **364**: 272−275.

[9] Wang, X., Liu, J. J. 2019. Analyses of the environmental characteristics of asteroids and the current research state. *Spacecraft Environment Engineering*, **36**(6): 533−541 (in Chinese).

[10] de la Fuente Marcos, C., de la Fuente Marcos, R. 2016. Asteroid(469219) 2016HO$_3$, the smallest and closet earth quasi-satellites. *Monthly Notices of the Royal Astronomical Society*, **462**(4): 3441−3456.

[11] Wang, Y. B. 2017. Observational study of photometric phase curves of asteroids. Doctor thesis, Yunnan Observatories, Chinese Academy of Sciences. (in Chinese)

[12] MPC. 2016. IAU minor planet center. https://minorplanet center.net/db_search/showobject?object_id=469219.

[13] Fohring, D., Reddy, V., Wainscoat, R., et al. 2018. Photometry and spectroscopy of (469129) 2016HO$_3$. In Division for Planetary Sciences Meeting.

[14] Sharkey, B. N. L., Reddy, V., Malhotra, R., et al. 2021. Lunar-like Silicate material forms the Earth quasi-satellite (469219) 2016HO$_3$ Kamo'oalewa. *Commucation Earth & Environment* , 231.

[15] Delbo, M., Harris, A. W. 2002. Physical properties of near-Earth asteroids from thermal infrared observations and thermal modeling. *Meteoritics & Planet Science*, **37**(12): 1929−1936.

[16] Barnouin-Jha, O. S., Cheng, A. F., Mukai, T., et al. 2008. Small-scale topography of 25143 Itokawa from the Hayabusa laser altimeter. *Icarus*, **198**(1): 108−124.

[17] Liu, W., Yan, J. G., Li, F., et al. 2017. Estimation on the regolith thickness distribution and the surface strength of 433-Eros. *Progress in Geophysics*, **32**(6): 2353−2359.(in Chinese)

[18] Huang, C. Y., Yu, Y., Guo, F., et al. 2021. Structural Stability of (469219)KAMO' OALEWA: Dependencies on Material Parameters. In the 7th IAA Planetary Defense Conference.